Minimal Hubbard models of maximal Hilbert space fragmentation

Yves H. Kwan,[1] Patrick H. Wilhelm,[2] Sounak Biswas,[3] and S.A. Parameswaran[4]

[1] *Princeton Center for Theoretical Science, Princeton University, Princeton NJ 08544, USA*
[2] *Institut für Theoretische Physik, Universität Innsbruck, A-6020 Innsbruck, Austria*
[3] *Institut für Theoretische Physik und Astrophysik, Universität Würzburg, 97074 Würzburg, Germany*
[4] *Rudolf Peierls Centre for Theoretical Physics, Parks Road, Oxford, OX1 3PU, UK*

We show that Hubbard models with nearest-neighbor hopping and a nearest-neighbor hardcore constraint exhibit 'maximal' Hilbert space fragmentation in many lattices of arbitrary dimension d. Focusing on the $d = 1$ rhombus chain and the $d = 2$ Lieb lattice, we demonstrate that the fragmentation is *strong* for all fillings in the thermodynamic limit, and explicitly construct all emergent integrals of motion, which include an extensive set of higher-form symmetries. Blockades consisting of frozen particles partition the system in real space, leading to anomalous dynamics. Our results are potentially relevant to optical lattices of dipolar and Rydberg-dressed atoms.

Introduction.—Thermalization in closed quantum many-body systems has recently garnered increasing attention, partly spurred by advances in experimental platforms and quantum simulators [1–11]. While many-body localized [12, 13] and integrable [14] systems have been long known as exceptions that break ergodicity, Hilbert space fragmentation [15] has emerged as a new route to violating the eigenstate thermalization hypothesis (ETH) [16–18]. Here, additional symmetries or constraints cause the Hamiltonian or time evolution operator to fracture into exponentially many dynamically disconnected blocks. As a result, even within a symmetry sector, such systems exhibit anomalous thermalization. The earliest examples involved mobility restrictions due to the combination of charge and dipole conservation [19–22], but fragmentation has been subsequently uncovered in a wide variety of settings [23–57].

Kinematic constraints often arise naturally from strong correlations. For example, the t-J model that forbids doublon occupancy is the strong-coupling limit of the Hubbard model, while the PXP model emerges within the blockaded subspace in Rydberg arrays. The low-energy properties of these and related Hamiltonians have been studied as settings for correlated and topological phenomena, and various one-dimensional versions have been shown to exhibit fragmentation and quantum many-body scars [21, 24, 25, 27, 30, 31, 49, 58].

In this paper, we study Hilbert space fragmentation in spinless extended Hubbard models of strongly-interacting fermions or bosons with short-range hopping on general lattices. In the limit of infinite nearest-neighbor interactions V_1, their effects are encoded in kinematic constraints that forbid nearest-neighbor occupancy of particles. Focusing on two representative lattices, the rhombus chain and the Lieb lattice, we explicitly construct all emergent integrals of motion and demonstrate the existence of strong fragmentation for all fillings through analytical and numerical arguments. The non-trivial physics arises from an intuitive real-space picture of blockades which partition the system into disconnected subregions.

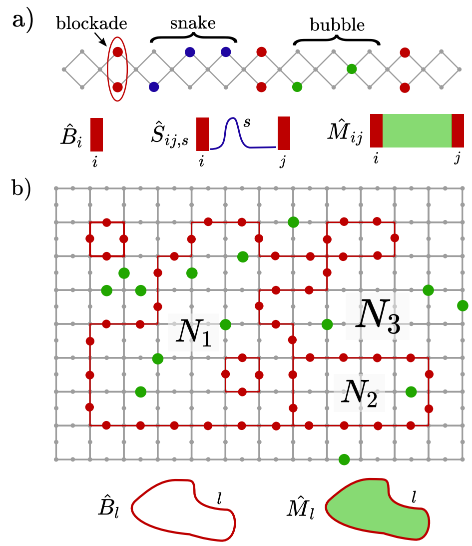

FIG. 1. **Fragmention in extended hardcore Hubbard models.** a) Blockades in the rhombus chain are formed by two particles (red) on opposite corners, and demarcate frozen 'snakes' (blue) and bubbles of mobile particles (green). b) Blockades on the Lieb lattice are due to closed frozen loops (red) of occupied particles on Lieb sites, which create bubbles with emergent subsystem charges N_1, N_2, N_3. For both lattices, commutant algebra generators are schematically shown.

In contrast to many previous studies of fragmentation, our model has a single global $U_c(1)$ symmetry corresponding to particle conservation, and is relevant for lattices in arbitrary dimensions $d \geq 1$. We discuss consequences for anomalous dynamics and thermalization, generalizations to other lattices and settings, and assess the suitability of existing platforms involving dipolar or Rydberg-dressed atoms as settings for such phenomena.

Model.—We consider a model of N_p interacting spinless fermions or bosons on the N_s sites of a graph in arbitrary dimensions. The filling factor is defined as $\nu = N_p/N_s$. Two key requirements are the restriction to nearest-neighbor (n.n.) hopping, and an extended hardcore constraint that prevents two particles from occupying the same or adjacent sites. The Hamiltonian is then

$$\hat{H} = \sum_i w_i \hat{d}_i^\dagger \hat{d}_i - \sum_{\langle i,j \rangle} t_{ij} \hat{d}_i^\dagger \hat{d}_j + \sum_{ij} V_{ij} \hat{n}_i \hat{n}_j, \quad (1)$$

where $\hat{n} = \hat{c}_i^\dagger \hat{c}_i$, and $\hat{d}_i^\dagger = \hat{c}_i^\dagger \prod_{\langle j,i \rangle}(1 - \hat{n}_j)$ is the dressed creation operator which acts within the hardcore subspace. The interaction V_{ij} can be of arbitrary range, and the general site-dependence of the parameters means that the only conventional symmetry is the $U_c(1)$ corresponding to the global conserved charge $\hat{N} = N_p$.

For many lattices and fillings, Eq. 1 is *fragmented* in the Fock basis, meaning that the Hamiltonian retains a non-trivial block-diagonal structure even when restricted to a symmetry sector labelled by N_p. In other words, the symmetry-resolved Hilbert subspace of dimension D_{sym} decomposes into smaller Krylov fragments $\mathcal{K}_\alpha$ of size $\dim(\mathcal{K}_\alpha)$, each of which are closed under Hamiltonian time evolution. The origin of this phenomenon lies in frozen subsets of particles which are completely immobile due to the hardcore constraint (e.g. red pairs in Fig. 1a). In many cases, these frozen regions are *blockades* that do not allow transmission of particles, and hence partition the system into disconnected *bubbles* each of which has a conserved subsystem charge (see Fig. 1b). Each bubble can contain mobile particles and further nested blockades. Fragments with distinct blockade networks and bubble charges cannot be connected by $\hat{H}$. As shown later, the fragmentation structure is characterized by a hierarchy of emergent higher-form symmetries.

Rhombus chain.—Our first example lattice is the $d = 1$ rhombus chain (RC) with L unit cells (see also the 'spin lace' model in Ref. [59]), each of which contains two corner sites '$\wedge, \vee$' and one junction site '$\times$' (Fig. 1a). The maximum allowed filling is $\nu = 2/3$. Two particles on opposite corner sites comprise a blockade. Between two consecutive blockades, there is either a bubble region of mobile particles, or a string of frozen particles dubbed a snake. Within a global charge sector, a Krylov fragment can be uniquely identified by specifying the blockade positions, and the intervening snake configurations and bubble charges.

This physics is succinctly captured by the commutant algebra $\mathcal{C}$, which Ref. [23] used to characterize the fragmented structure shared by families of models. $\mathcal{C}$ consists of all operators which commute with every term of $\hat{H}$. Besides the trivial identity operator $\mathbb{1}$, the global $U_c(1)$ provides the usual symmetry algebra consisting of functionally independent powers of $\hat{N}$: there are $\mathcal{O}(L)$ such combinations, consistent with a continuous global symmetry. We now turn to the novel integrals of motion (IOMs) (Fig. 1a, bottom). For simplicity, we ignore boundary effects below. Individual blockades can be diagnosed by a set of projectors $\hat{B}_i = \hat{n}_{i\wedge}\hat{n}_{i\vee}$ onto pairs of occupied rhombus corners. Snakes are detected by operators $\hat{S}_{ij,s} = \hat{B}_i \hat{B}_j \prod_{i<k<j} \hat{n}_{k,s_k}(1 - \hat{n}_{k,\bar{s}_k})$, where s is a string of $\wedge, \vee$ of length $j - i - 1$ and $\bar{s}_k$ indicates the opposite corner. Similarly, charges within bubbles are denoted $\hat{M}_{ij} = \hat{B}_i \hat{B}_j \sum_{i<k<j} \hat{n}_k$. Note that $\hat{S}_{ij,s}, \hat{M}_{ij}$ are non-locally conditioned operators which are only active if the blockades are present. A generating set for the commutant algebra for the RC is

$$\text{gen}(\mathcal{C}) = \{\mathbb{1}, \hat{N}, \hat{P}_\times, \{\hat{B}_i\}, \{\hat{S}_{ij,s}\}, \{\hat{M}_{ij}\}\} \quad (2)$$

where we have also included the projector $\hat{P}_\times$ onto the frozen $\nu = 1/3$ state with all junction sites filled. Since $\mathcal{C}$ is Abelian, the fragmentation is 'classical' and hence manifest in a product basis (the Fock states) [23]. $\dim(\mathcal{C})$ gives the total number of Krylov subspaces across all N_p sectors. The algebra generated by Eq. 2 provides the entire structure of emergent IOMs. Evidently, this grows exponentially with system size as there are at least 2^L individual snake operators alone.

Lieb lattice.—We now turn to the square Lieb lattice (SLL) of N unit cells, which provides the simplest example of extensive fragmentation [60] in $d = 2$. Each unit cell contains one square lattice site and two 'Lieb' sites on the links, and the maximum filling consistent with the hardcore constraint is $\nu = 2/3$. Blockades can be introduced by drawing arbitrary closed loops on the links of the square lattice, and placing particles on all of the Lieb sites that are traversed (Fig. 1b). Primitive blockades, which cannot be decomposed into smaller ones, are equivalent to self-avoiding polygons on the square lattice (a similar blockade-loop-structure also occurs in height-conserving dimer models [42]). The smallest blockade is a single plaquette with four Lieb particles. Note that unlike in $O(n)$ loop models, loops are allowed to share edges and intersect. The configuration of loops divides the system into bubbles with conserved subsystem charges.

As in the RC, we can construct extended operators which diagnose the Krylov fragments. Neglecting boundary effects for simplicity, we define loop blockade projectors $\hat{B}_l = \prod_{\text{Lieb } i \in l} \hat{n}_i$, where the product is over Lieb sites on loop l. For each loop, we also define the membrane operator $\hat{M}_l = \hat{B}_l \sum_{i \in b(l)} \hat{n}_i$ which counts the charge inside a bubble $b(l)$ conditioned on the existence of a surrounding blockade. These operators have support on a line contour and are examples of one-form symmetries (Fig. 1b), though they are only non-vanishing on Krylov subspaces that contain the corresponding blockade. The commutant algebra for the SLL is generated by

$$\text{gen}(\mathcal{C}) = \{\mathbb{1}, \hat{N}, \hat{P}_{\text{sq.}}, \{\hat{B}_l\}, \{\hat{M}_l\}\} \quad (3)$$

where $\hat{P}_{\text{sq.}}$ is the projector onto the frozen $\nu = 1/3$ state with all square lattice sites filled. The number of fragments is exponential (since, e.g. counting products of single-plaquette loop operators alone gives 2^N possibilities). With periodic boundary conditions (PBCs), there are also non-contractible loop operators. The associated

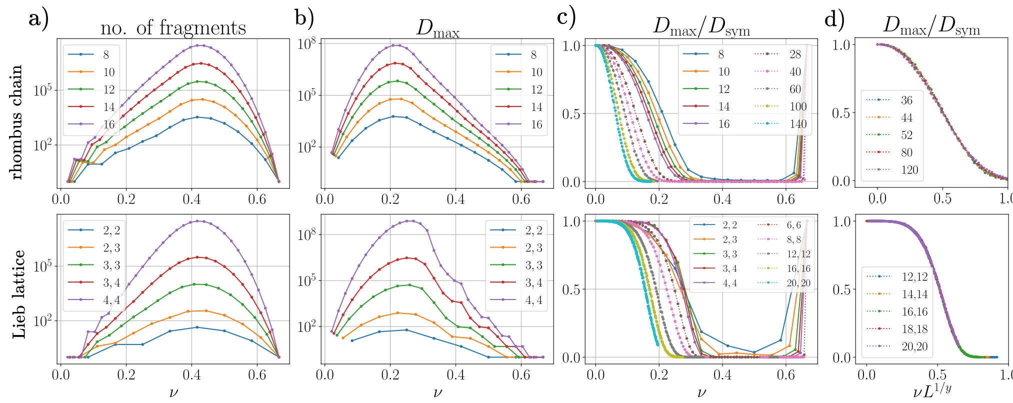

FIG. 2. **Exact enumeration (EE) and Monte Carlo (MC) sampling of fragments.** Top (bottom) row indicates results on L ($N_x \times N_y$) unit cells of the rhombus chain (Lieb lattice) with periodic boundary conditions. a) Number of fragments in EE for each filling factor ν. b) Dimension of largest Krylov fragment $D_{\max}$ in EE. c) Ratio of $D_{\max}$ to the dimension of the total symmetry sector $D_{\rm sym}$. There is a finite-size drift $D_{\max}/D_{\rm sym} \to 0$, suggesting that the system is strongly-fragmented for all fillings in the thermodynamic limit. Solid (dotted) lines refer to EE (MC) data. All MC data points include at least 3000 samples. d) Scaling collapse of MC data for $D_{\max}/D_{\rm sym}$ as a function of $(\nu - \nu_c)L^{1/y}$ with fixed $\nu_c = 0$, and fitted exponents $y = 2.4(1)$ ($y = 2.5(1)$) for the rhombus chain (Lieb lattice).

membrane operators count the charge between two such loops with identical winding numbers.

Strong fragmentation.—While we have demonstrated an exponential number of fragments for the RC and SLL, their dimensions and distribution across different N_p sectors is not yet clear. To understand the extent of ergodicity breaking, it is useful to contrast *strong* and *weak* fragmentation [19, 20]. Within a conventional symmetry sector (i.e. filling factor ν in the thermodynamic limit), a system is strongly fragmented if the size of the largest fragment $D_{\max} = \max_\alpha\{\dim(\mathcal{K}_\alpha)\}$ is a vanishing fraction of $D_{\rm sym}$ as the number of unit cells $N \to \infty$. On the other hand, $D_{\max}/D_{\rm sym} \to 1$ for weak fragmentation, where typical states are expected to look thermal [15]. It is natural that strong fragmentation, if it exists, occurs at larger fillings where there are likely more blockades and smaller bubbles. In fact, we demonstrate via cluster expansion techniques [61–63] that there is strong fragmentation $D_{\max}/D_{\rm sym} \sim \exp(-cN\nu^s)$ as $\nu \to 0$ in the thermodynamic limit, with s set by the number of particles in the smallest blockade. The exponential is reminiscent of the finite-size scaling form for an incipient phase transition at $\nu = 0^+$, with a correlation volume growing as $\sim \nu^{-s}$.

To understand more quantitatively the distribution of fragments and the strong/weak phase diagram, we perform an exact depth-first enumeration (EE) of fragments [63, 64]. As shown in Fig. 2 for PBCs, the number of fragments is exponential in system volume for most fillings. $D_{\max}/D_{\rm sym}$ for the RC shows clear size-dependence, suggesting a drift of the weak-to-strong crossover ν_c towards lower fillings, but the data for SLL are more difficult to interpret due to finite-size effects.

While EE provides full information on the fragments for finite systems, it is quickly limited by the exponential growth of the Hilbert space. Therefore, we use Monte Carlo (MC) sampling to follow the ν-dependence of the weak-strong crossover to larger systems (see Ref. [63] for details of the algorithm). As shown in Fig. 2c, the data show a clear drift of the weak-strong crossover to lower fillings. A scaling collapse strongly suggests that the critical filling $\nu_c = 0$ in the thermodynamic limit (Fig. 2d), implying strong fragmentation for all fillings, though the best fit exponents indicate the presence of significant finite-size effects.

Thermalization and localization.—Strong fragmentation leads to violation of the weak form of ETH within each global particle number sector [15]. Local observables such as the density can differ dramatically for nearby states in the middle of the spectrum. For instance, the site i may be part of a blockade in one eigenstate so that $\langle \hat{n}_i \rangle = 1$, but part of a dilute thermal bubble for another eigenstate at the same energy density. The bipartite entanglement entropy vanishes in fragments where the entanglement cut traverses a blockade whose width is sufficiently larger than the interaction range, and is generally much lower than the Page value, while level spacings are expected to follow a Poisson distribution.

Despite the ergodicity-breaking outlined above, one may ask whether individual Krylov subspaces are themselves thermal [21]. The answer depends on the fragment and the range of interactions. Consider the fragment on the Lieb lattice that is represented in Fig. 1b which has bubbles b_l with corresponding conserved charges N_l. For $V_{ij} = 0$ (i.e. the only interactions are the hardcore constraints), the bubbles do not interact with each other. We therefore have isolated subsystems that can realize various physics depending on their disorder, dimension-

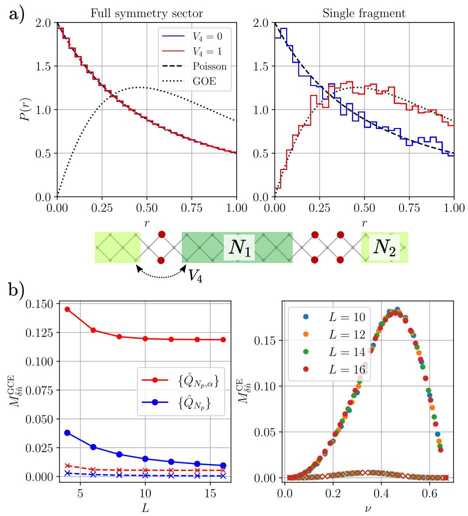

FIG. 3. **Thermalization and dynamics in the rhombus chain.** a) Left: Distribution $P(r)$ of level spacing ratios r for symmetry sector $L=12, N_p=13$, showing Poisson statistics. Right: $P(r)$ for the two-bubble fragment shown at bottom with emergent charges $N_1=4, N_2=3$, showing the change from Poisson to GOE statistics on including horizontal-range-4 (V_4) interactions. b) Mazur bounds for the dynamical autocorrelator of $\delta\hat{n}_i = \hat{n}_i - \langle n \rangle_i$. Left: Red (blue) indicates bounds in the grand canonical ensemble, taking into account fragmentation (only N_p conservation). Circles (crosses) indicate the $\wedge$ ($\times$) sublattice. Right: Bounds obtained using fragmentation in the canonical ensemble.

ality, and charge. Sufficiently disordered 1d bubbles may be Anderson or many-body localized, while large 2d bubbles are expected to locally satisfy ETH, but the fragment overall fails to equilibrate. As interactions V_{ij} of progressively longer range are introduced, the bubbles begin to interact and thermalize each other, and only bubbles with sufficiently thick 'shielding' boundaries remain isolated. For infinite-range interactions, we expect Krylov-restricted thermalization to occur for all fragments. We demonstrate this in the RC by using exact diagonalization (ED) to compute the distribution of level spacings $r = \frac{\min(s_n, s_{n-1})}{\max(s_n, s_{n-1})}$ [65, 66], where $s_n = E_{n+1} - E_n$. Fig. 3a shows that a typical fixed-N_p sector exhibits Poisson statistics. However, an individual fragment in that sector can cross over from Poisson to Gaussian orthgonal ensemble (GOE) statistics as V_4 is increased.

The presence of blockades influences the nature of transport and dynamics in these models. While long-range interactions permit bubbles to transmit information, particle exchange remains forbidden. The propagator $\langle \hat{c}_i^\dagger \hat{c}_j \rangle$ vanishes in fragments where i, j belong to different bubbles. Even if there is a percolating mobile region, other bubbles act as scatterers, possibly with internal degrees of freedom, that may hinder charge transport. The fragmentation also contributes to a lower (Mazur) bound $M_{\delta\hat{n}}$ on the infinite-temperature dynamical charge autocorrelation function [23, 63]

$$\lim_{\tau\to\infty} \frac{1}{\tau} \int_0^\tau dt \langle \delta\hat{n}_i(t)\delta\hat{n}_i(0)\rangle \geq M_{\delta\hat{n}}, \tag{4}$$

where $\delta\hat{n}_i = \hat{n}_i - \langle \hat{n}_i \rangle$ is traceless. This can be extracted using EE, as detailed in Ref. [63]. As shown for the RC in Fig. 3b (and for the SLL in [63]), in the grand canonical ensemble, the global $U_c(1)$ symmetry only constrains $M_{\delta\hat{n}} \sim 1/L$, but the bound saturates to a finite value when accounting for the fragmented structure. Similar behavior occurs within a fixed-N_p sector, where the only contributions to $M_{\delta\hat{n}}$ arise from the emergent symmetries. The bound is stronger for sublattices that participate in blockades, since such charges cannot relax at all.

Extensions.—We can relax the extended hardcore constraint while taking the n.n. interaction $V_1 \to \infty$, such that the number of occupied n.n. bonds is a conserved [24, 49]. A pair of n.n. particles remains frozen unless a third particle approaches and enables a resonant hop (if V_1 is uniform), but blockades remain frozen and impenetrable. Similarly, we can relax the onsite constraint and reintroduce spins, while preserving the blockade physics. For finite n.n. interactions, strictly speaking the fragmentation disappears completely as now it is possible for particles to pass through a blockade, or for the blockade to melt. However for large V_1, the fragmentation is still expected to leave an imprint on dynamics since the effective n.n.n. hopping that is generated is suppressed as $\sim t^2/V_1$. Thicker blockades will take longer to break down. Similar comments apply to longer-range hoppings: while typically exponentially suppressed, they make the emergent conservation laws only approximate. In these cases, the dynamics may show features of fragmentation at short times, but these are eventually washed out as $t \to \infty$.

In 2d, strong fragmentation is possible in other graphs which allow for finite blockades [63]. In fact, any 2d graph can be converted into one that hosts blockade loops by inserting 'Lieb' sites in the middle of every edge. Other lattices, such as the square and honeycomb lattices, have blockades which must span the system size [63], and hence are expected to be weakly fragmented for all ν (though they may exhibit a finite-size strong-weak crossover [44]). Higher-dimensional generalizations are possible, where the formation of bubbles with subregion charge conservation requires closed $(d-1)$-dimensional blockade hypersurfaces. In Ref. [63], we also discuss the possibility of further fragmentation in a non-diagonal basis for appropriately tuned couplings.

We propose that the physics here can be probed in existing experimental platforms that realize extended variants of the (Bose)-Hubbard model [67–69]. The nontrivial requirement is the generation of desired lattices and sufficiently strong onsite and n.n. interactions. Ideally, the interaction falls off rapidly beyond n.n. range so that dynamical processes within the bubbles are not energetically suppressed. Various potentials like the Lieb lattice have been experimentally realized in optical lattices of ultracold gases [70–74]. Dipolar atoms or molecules with power-law decaying V_{ij} can provide the required hierarchy of couplings when combined with tuning of the hopping strengths [75–82]. Similarly, Rydberg-dressed atoms inherit a strong repulsion within a tunable blockade radius and long-range r^{-6} falloff [83–89]. The temperature can be comparable to the couplings, as long as it is much less than V_1. While existing experiments have investigated fragmentation in tilted Hubbard models [90, 91], we emphasize that the systems introduced in this work are qualitatively distinct in several aspects. Our hardcore models, which exhibit strong fragmentation for all fillings, do not rely on tilting to induce resonant hopping processes or an emergent dipole conservation. In addition, the non-ergodic dynamics can be isotropic, and is robust to disordered couplings and arbitrary-range density-density interactions.

Conclusions and outlook.—The combination of nearest-neighbor hoppings and extended hardcore constraint in Hubbard models induces Hilbert space fragmentation in many lattices of different dimensions. Frozen blockade regions inhibit charge transfer between emergent bubbles, and lead to an exponential hierarchy of integrals of motion. The necessary ingredients for realizing such ergodicity-breaking are already present in current experimental platforms such as ultracold atomic gases in optical lattices. While we have focused on two examples that exhibit strong fragmentation for all fillings, it would be interesting to study the extent of fragmentation and the scaling behavior of $D_{\text{max}}/D_{\text{sym}}$ in other physically relevant lattices. For rational couplings, investigating quantum fragmentation [23] via integer polynomial factorization [92] is another interesting direction. We leave to future work the question of how the anomalous dynamics in these models survives the inclusion of perturbations that lift the fragmentation structure.

Acknowledgements.—We thank Andrei Bernevig, Sarang Gopalakrishnan, Zhaoyu Han, Vedika Khemani, Steve Kivelson, Abhinav Prem, and Nicolas Regnault for useful discussions. We acknowledge support from the European Research Council (ERC) under the European Union Horizon 2020 Research and Innovation Programme (Grant Agreement Nos. 804213-TMCS), EPSRC grant EP/S020527/1, and the Austrian Science Fund FWF within the DK-ALM (W1259-N27). Statement of compliance with EPSRC policy framework on research data: This publication is theoretical work that does not require supporting research data.

[1] T. Kinoshita, T. Wenger, and D. S. Weiss, A quantum newton's cradle, Nature **440**, 900 (2006).

[2] M. Gring, M. Kuhnert, T. Langen, T. Kitagawa, B. Rauer, M. Schreitl, I. Mazets, D. A. Smith, E. Demler, and J. Schmiedmayer, Relaxation and prethermalization in an isolated quantum system, Science **337**, 1318 (2012).

[3] S. Trotzky, Y.-A. Chen, A. Flesch, I. P. McCulloch, U. Schollwöck, J. Eisert, and I. Bloch, Probing the relaxation towards equilibrium in an isolated strongly correlated one-dimensional bose gas, Nature Physics **8**, 325 (2012).

[4] M. Schreiber, S. S. Hodgman, P. Bordia, H. P. Lüschen, M. H. Fischer, R. Vosk, E. Altman, U. Schneider, and I. Bloch, Observation of many-body localization of interacting fermions in a quasirandom optical lattice, Science **349**, 842 (2015).

[5] J. yoon Choi, S. Hild, J. Zeiher, P. Schauß, A. Rubio-Abadal, T. Yefsah, V. Khemani, D. A. Huse, I. Bloch, and C. Gross, Exploring the many-body localization transition in two dimensions, Science **352**, 1547 (2016).

[6] A. M. Kaufman, M. E. Tai, A. Lukin, M. Rispoli, R. Schittko, P. M. Preiss, and M. Greiner, Quantum thermalization through entanglement in an isolated many-body system, Science **353**, 794 (2016).

[7] J. Smith, A. Lee, P. Richerme, B. Neyenhuis, P. W. Hess, P. Hauke, M. Heyl, D. A. Huse, and C. Monroe, Many-body localization in a quantum simulator with programmable random disorder, Nature Physics **12**, 907 (2016).

[8] H. Bernien, S. Schwartz, A. Keesling, H. Levine, A. Omran, H. Pichler, S. Choi, A. S. Zibrov, M. Endres, M. Greiner, V. Vuletić, and M. D. Lukin, Probing many-body dynamics on a 51-atom quantum simulator, Nature **551**, 579 (2017).

[9] G. Kucsko, S. Choi, J. Choi, P. Maurer, H. Zhou, R. Landig, H. Sumiya, S. Onoda, J. Isoya, F. Jelezko, E. Demler, N. Yao, and M. Lukin, Critical thermalization of a disordered dipolar spin system in diamond, Physical Review Letters **121**, 10.1103/physrevlett.121.023601 (2018).

[10] W. Morong, F. Liu, P. Becker, K. S. Collins, L. Feng, A. Kyprianidis, G. Pagano, T. You, A. V. Gorshkov, and C. Monroe, Observation of stark many-body localization without disorder, Nature **599**, 393 (2021).

[11] S. Scherg, T. Kohlert, P. Sala, F. Pollmann, B. H. Madhusudhana, I. Bloch, and M. Aidelsburger, Observing non-ergodicity due to kinetic constraints in tilted fermi-hubbard chains, Nature Communications **12**, 10.1038/s41467-021-24726-0 (2021).

[12] R. Nandkishore and D. A. Huse, Many-body localization and thermalization in quantum statistical mechanics, Annual Review of Condensed Matter Physics **6**, 15 (2015).

[13] D. A. Abanin, E. Altman, I. Bloch, and M. Serbyn, Colloquium : Many-body localization, thermalization, and entanglement, Reviews of Modern Physics **91**, 10.1103/revmodphys.91.021001 (2019).

[14] M. Rigol, V. Dunjko, V. Yurovsky, and M. Olshanii, Relaxation in a completely integrable many-body quantum system: An ab initio study of the dynamics of the highly excited states of 1d lattice hard-core bosons, Physical Review Letters **98**, 10.1103/physrevlett.98.050405 (2007).

[15] S. Moudgalya, B. A. Bernevig, and N. Regnault, Quantum many-body scars and hilbert space fragmentation: a review of exact results, Reports on Progress in Physics **85**, 086501 (2022).

[16] J. M. Deutsch, Quantum statistical mechanics in a closed system, Physical Review A **43**, 2046 (1991).

[17] M. Srednicki, Chaos and quantum thermalization, Physical Review E **50**, 888 (1994).

[18] M. Rigol, V. Dunjko, and M. Olshanii, Thermalization and its mechanism for generic isolated quantum systems, Nature **452**, 854 (2008).

[19] P. Sala, T. Rakovszky, R. Verresen, M. Knap, and F. Pollmann, Ergodicity breaking arising from hilbert space fragmentation in dipole-conserving hamiltonians, Physical Review X **10**, 10.1103/physrevx.10.011047 (2020).

[20] V. Khemani, M. Hermele, and R. Nandkishore, Localization from hilbert space shattering: From theory to physical realizations, Physical Review B **101**, 10.1103/physrevb.101.174204 (2020).

[21] S. Moudgalya, A. Prem, R. Nandkishore, N. Regnault, and B. A. Bernevig, Thermalization and its absence within krylov subspaces of a constrained hamiltonian, in *Memorial Volume for Shoucheng Zhang* (WORLD SCIENTIFIC, 2021) pp. 147–209.

[22] S. Pai, M. Pretko, and R. M. Nandkishore, Localization in fractonic random circuits, Physical Review X **9**, 10.1103/physrevx.9.021003 (2019).

[23] S. Moudgalya and O. I. Motrunich, Hilbert space fragmentation and commutant algebras, Physical Review X **12**, 10.1103/physrevx.12.011050 (2022).

[24] G. D. Tomasi, D. Hetterich, P. Sala, and F. Pollmann, Dynamics of strongly interacting systems: From fock-space fragmentation to many-body localization, Physical Review B **100**, 10.1103/physrevb.100.214313 (2019).

[25] T. Rakovszky, P. Sala, R. Verresen, M. Knap, and F. Pollmann, Statistical localization: From strong fragmentation to strong edge modes, Physical Review B **101**, 10.1103/physrevb.101.125126 (2020).

[26] A. Morningstar, V. Khemani, and D. A. Huse, Kinetically constrained freezing transition in a dipole-conserving system, Physical Review B **101**, 10.1103/physrevb.101.214205 (2020).

[27] I.-C. Chen and T. Iadecola, Emergent symmetries and slow quantum dynamics in a rydberg-atom chain with confinement, Physical Review B **103**, 10.1103/physrevb.103.214304 (2021).

[28] Z.-C. Yang, F. Liu, A. V. Gorshkov, and T. Iadecola, Hilbert-space fragmentation from strict confinement, Physical Review Letters **124**, 10.1103/physrevlett.124.207602 (2020).

[29] A. Bastianello, U. Borla, and S. Moroz, Fragmentation and emergent integrable transport in the weakly tilted ising chain, Physical Review Letters **128**, 10.1103/physrevlett.128.196601 (2022).

[30] B. Mukherjee, Z. Cai, and W. V. Liu, Constraint-induced breaking and restoration of ergodicity in spin-1 PXP models, Physical Review Research **3**, 10.1103/physrevresearch.3.033201 (2021).

[31] B. Mukherjee, D. Banerjee, K. Sengupta, and A. Sen, Minimal model for hilbert space fragmentation with local constraints, Physical Review B **104**, 10.1103/physrevb.104.155117 (2021).

[32] K. Lee, A. Pal, and H. J. Changlani, Frustration-induced emergent hilbert space fragmentation, Physical Review B **103**, 10.1103/physrevb.103.235133 (2021).

[33] D. Hahn, P. A. McClarty, and D. J. Luitz, Information dynamics in a model with hilbert space fragmentation, SciPost Physics **11**, 10.21468/scipostphys.11.4.074 (2021).

[34] W.-H. Li, X. Deng, and L. Santos, Hilbert space shattering and disorder-free localization in polar lattice gases, Physical Review Letters **127**, 10.1103/physrevlett.127.260601 (2021).

[35] L. Zadnik and M. Fagotti, The folded spin-1/2 XXZ model: I. diagonalisation, jamming, and ground state properties, SciPost Physics Core **4**, 10.21468/scipostphyscore.4.2.010 (2021).

[36] L. Zadnik, K. Bidzhiev, and M. Fagotti, The folded spin-1/2 XXZ model: II. thermodynamics and hydrodynamics with a minimal set of charges, SciPost Physics **10**, 10.21468/scipostphys.10.5.099 (2021).

[37] B. Pozsgay, T. Gombor, A. Hutsalyuk, Y. Jiang, L. Pristyák, and E. Vernier, Integrable spin chain with hilbert space fragmentation and solvable real-time dynamics, Physical Review E **104**, 10.1103/physreve.104.044106 (2021).

[38] A. Khudorozhkov, A. Tiwari, C. Chamon, and T. Neupert, Hilbert space fragmentation in a 2d quantum spin system with subsystem symmetries, SciPost Physics **13**, 10.21468/scipostphys.13.4.098 (2022).

[39] C. M. Langlett and S. Xu, Hilbert space fragmentation and exact scars of generalized fredkin spin chains, Physical Review B **103**, 10.1103/physrevb.103.l220304 (2021).

[40] J. Richter and A. Pal, Anomalous hydrodynamics in a class of scarred frustration-free hamiltonians, Physical Review Research **4**, 10.1103/physrevresearch.4.l012003 (2022).

[41] P. Brighi, M. Ljubotina, and M. Serbyn, Hilbert space fragmentation and slow dynamics in particle-conserving quantum east models (2022).

[42] Z. Yan, Z. Y. Meng, D. A. Huse, and A. Chan, Height-conserving quantum dimer models, Physical Review B **106**, 10.1103/physrevb.106.l041115 (2022).

[43] A. Yoshinaga, H. Hakoshima, T. Imoto, Y. Matsuzaki, and R. Hamazaki, Emergence of hilbert space fragmentation in ising models with a weak transverse field, Physical Review Letters **129**, 10.1103/physrevlett.129.090602 (2022).

[44] O. Hart and R. Nandkishore, Hilbert space shattering and dynamical freezing in the quantum ising model, Physical Review B **106**, 10.1103/physrevb.106.214426 (2022).

[45] B. Lian, Quantum breakdown model: From many-body localization to chaos with scars, Physical Review B **107**, 10.1103/physrevb.107.115171 (2023).

[46] P. Karpov, R. Verdel, Y.-P. Huang, M. Schmitt, and M. Heyl, Disorder-free localization in an interacting 2d lattice gauge theory, Physical Review Letters **126**, 10.1103/physrevlett.126.130401 (2021).

[47] N. Chakraborty, M. Heyl, P. Karpov, and R. Moessner, Spectral response of disorder-free localized lattice gauge theories (2022).

[48] N. Chakraborty, M. Heyl, P. Karpov, and R. Moessner, Disorder-free localization transition in a two-dimensional lattice gauge theory, arXiv 10.48550/ARXIV.2203.06198 (2022).

[49] P. Frey, L. Hackl, and S. Rachel, Hilbert space fragmentation and interaction-induced localization in the ex-

tended fermi-hubbard model, Physical Review B **106**, 10.1103/physrevb.106.l220301 (2022).
[50] D. T. Stephen, O. Hart, and R. M. Nandkishore, Ergodicity breaking provably robust to arbitrary perturbations (2022).
[51] H. Zhao, J. Vovrosh, F. Mintert, and J. Knolle, Quantum many-body scars in optical lattices, Physical Review Letters **124**, 10.1103/physrevlett.124.160604 (2020).
[52] H. Zhao, A. Smith, F. Mintert, and J. Knolle, Orthogonal quantum many-body scars, Physical Review Letters **127**, 10.1103/physrevlett.127.150601 (2021).
[53] A. Chattopadhyay, B. Mukherjee, K. Sengupta, and A. Sen, Strong hilbert space fragmentation via emergent quantum drums in two dimensions (2022).
[54] M. Borsi, L. Pristyák, and B. Pozsgay, Matrix product symmetries and breakdown of thermalization from hard rod deformations (2023).
[55] B. Buča, Out-of-time-ordered crystals and fragmentation, Physical Review Letters **128**, 10.1103/physrevlett.128.100601 (2022).
[56] B. Buča, Unified theory of local quantum many-body dynamics: Eigenoperator thermalization theorems (2023).
[57] E. Nicolau, A. M. Marques, J. Mompart, V. Ahufinger, and R. G. Dias, Local hilbert space fragmentation and weak thermalization in bose-hubbard diamond necklaces, Phys. Rev. B **107**, 094312 (2023).
[58] W.-H. Li, A. Dhar, X. Deng, and L. Santos, Cluster dynamics in two-dimensional lattice gases with intersite interactions, Physical Review A **103**, 10.1103/physreva.103.043331 (2021).
[59] B. Buca, A. Purkayastha, G. Guarnieri, M. T. Mitchison, D. Jaksch, and J. Goold, Quantum many-body attractors (2020).
[60] With the benefit of hindsight, the solvable limit of the Emery model on a similar lattice in Ref. 93 could be viewed as an early example of *subextensive* fragmentation.
[61] J. E. Mayer, The statistical mechanics of condensing systems. i, The Journal of Chemical Physics **5**, 67 (1937), https://doi.org/10.1063/1.1749933.
[62] S. Friedli and Y. Velenik, *Statistical Mechanics of Lattice Systems: A Concrete Mathematical Introduction* (Cambridge University Press, 2017).
[63] Y. H. Kwan, P. Wilhelm, S. Biswas, and S. A. Parameswaran, see supplementary material to this article, which also includes Refs. [94–97].
[64] N. G. Zhang and C. L. Henley, Stripes and holes in a two-dimensional model of spinless fermions or hardcore bosons, Phys. Rev. B **68**, 014506 (2003).
[65] V. Oganesyan and D. A. Huse, Localization of interacting fermions at high temperature, Phys. Rev. B **75**, 155111 (2007).
[66] Y. Y. Atas, E. Bogomolny, O. Giraud, and G. Roux, Distribution of the ratio of consecutive level spacings in random matrix ensembles, Phys. Rev. Lett. **110**, 084101 (2013).
[67] M. Lewenstein, A. Sanpera, V. Ahufinger, B. Damski, A. Sen(De), and U. Sen, Ultracold atomic gases in optical lattices: mimicking condensed matter physics and beyond, Advances in Physics **56**, 243 (2007).
[68] M. Lewenstein, A. Sanpera, and V. Ahufinger, *Ultracold Atoms in Optical Lattices: Simulating quantum many-body systems* (OUP Oxford, 2012).
[69] O. Dutta, M. Gajda, P. Hauke, M. Lewenstein, D.-S. Luhmann, B. A. Malomed, T. Sowinski, and J. Zakrzewski, Non-standard hubbard models in optical lattices: a review, Reports on Progress in Physics **78**, 066001 (2015).
[70] S. Taie, H. Ozawa, T. Ichinose, T. Nishio, S. Nakajima, and Y. Takahashi, Coherent driving and freezing of bosonic matter wave in an optical lieb lattice, Science Advances **1**, 10.1126/sciadv.1500854 (2015).
[71] H. Ozawa, S. Taie, T. Ichinose, and Y. Takahashi, Interaction-driven shift and distortion of a flat band in an optical lieb lattice, Physical Review Letters **118**, 10.1103/physrevlett.118.175301 (2017).
[72] R. Shen, L. B. Shao, B. Wang, and D. Y. Xing, Single dirac cone with a flat band touching on line-centered-square optical lattices, Physical Review B **81**, 10.1103/physrevb.81.041410 (2010).
[73] V. Apaja, M. Hyrkäs, and M. Manninen, Flat bands, dirac cones, and atom dynamics in an optical lattice, Physical Review A **82**, 10.1103/physreva.82.041402 (2010).
[74] S. Flannigan, L. Madail, R. G. Dias, and A. J. Daley, Hubbard models and state preparation in an optical lieb lattice, New Journal of Physics **23**, 083014 (2021).
[75] C. Trefzger, C. Menotti, B. Capogrosso-Sansone, and M. Lewenstein, Ultracold dipolar gases in optical lattices, Journal of Physics B: Atomic, Molecular and Optical Physics **44**, 193001 (2011).
[76] T. Lahaye, C. Menotti, L. Santos, M. Lewenstein, and T. Pfau, The physics of dipolar bosonic quantum gases, Reports on Progress in Physics **72**, 126401 (2009).
[77] B. Capogrosso-Sansone, C. Trefzger, M. Lewenstein, P. Zoller, and G. Pupillo, Quantum phases of cold polar molecules in 2d optical lattices, Physical Review Letters **104**, 10.1103/physrevlett.104.125301 (2010).
[78] M. A. Baranov, M. Dalmonte, G. Pupillo, and P. Zoller, Condensed matter theory of dipolar quantum gases, Chemical Reviews **112**, 5012 (2012).
[79] J. L. Bohn, A. M. Rey, and J. Ye, Cold molecules: Progress in quantum engineering of chemistry and quantum matter, Science **357**, 1002 (2017).
[80] S. A. Moses, J. P. Covey, M. T. Miecnikowski, D. S. Jin, and J. Ye, New frontiers for quantum gases of polar molecules, Nature Physics **13**, 13 (2016).
[81] S. Baier, M. J. Mark, D. Petter, K. Aikawa, L. Chomaz, Z. Cai, M. Baranov, P. Zoller, and F. Ferlaino, Extended bose-hubbard models with ultracold magnetic atoms, Science **352**, 201 (2016).
[82] L. Chomaz, I. Ferrier-Barbut, F. Ferlaino, B. Laburthe-Tolra, B. L. Lev, and T. Pfau, Dipolar physics: a review of experiments with magnetic quantum gases, Reports on Progress in Physics **86**, 026401 (2022).
[83] N. Henkel, R. Nath, and T. Pohl, Three-dimensional roton excitations and supersolid formation in rydberg-excited bose-einstein condensates, Physical Review Letters **104**, 10.1103/physrevlett.104.195302 (2010).
[84] G. Pupillo, A. Micheli, M. Boninsegni, I. Lesanovsky, and P. Zoller, Strongly correlated gases of rydberg-dressed atoms: Quantum and classical dynamics, Physical Review Letters **104**, 10.1103/physrevlett.104.223002 (2010).
[85] J. E. Johnson and S. L. Rolston, Interactions between rydberg-dressed atoms, Physical Review A **82**, 10.1103/physreva.82.033412 (2010).
[86] P. Schauß, J. Zeiher, T. Fukuhara, S. Hild, M. Cheneau,

T. Macrì, T. Pohl, I. Bloch, and C. Gross, Crystallization in ising quantum magnets, Science **347**, 1455 (2015).

[87] A. Browaeys and T. Lahaye, Many-body physics with individually controlled rydberg atoms, Nature Physics **16**, 132 (2020).

[88] E. Guardado-Sanchez, B. M. Spar, P. Schauss, R. Belyansky, J. T. Young, P. Bienias, A. V. Gorshkov, T. Iadecola, and W. S. Bakr, Quench dynamics of a fermi gas with strong nonlocal interactions, Physical Review X **11**, 10.1103/physrevx.11.021036 (2021).

[89] A. Dauphin, M. Müller, and M. A. Martin-Delgado, Quantum simulation of a topological mott insulator with rydberg atoms in a lieb lattice, Physical Review A **93**, 10.1103/physreva.93.043611 (2016).

[90] T. Kohlert, S. Scherg, P. Sala, F. Pollmann, B. Hebbe Madhusudhana, I. Bloch, and M. Aidelsburger, Exploring the regime of fragmentation in strongly tilted fermi-hubbard chains, Phys. Rev. Lett. **130**, 010201 (2023).

[91] D. Adler, D. Wei, M. Will, K. Srakaew, S. Agrawal, P. Weckesser, R. Moessner, F. Pollmann, I. Bloch, and J. Zeiher, Observation of hilbert-space fragmentation and fractonic excitations in two-dimensional hubbard systems (2024), arXiv:2404.14896 [cond-mat.quant-gas].

[92] N. Regnault and B. A. Bernevig, Integer characteristic polynomial factorization and hilbert space fragmentation (2022).

[93] S. A. Kivelson, E. Fradkin, and T. H. Geballe, Quasi-one-dimensional dynamics and nematic phases in the two-dimensional emery model, Phys. Rev. B **69**, 144505 (2004).

[94] M. Levin and C. P. Nave, Tensor renormalization group approach to two-dimensional classical lattice models, Physical Review Letters **99**, 10.1103/physrevlett.99.120601 (2007).

[95] Z.-C. Gu and X.-G. Wen, Tensor-entanglement-filtering renormalization approach and symmetry-protected topological order, Physical Review B **80**, 10.1103/physrevb.80.155131 (2009).

[96] G. W. Ford and G. E. Uhlenbeck, *Lectures in Statistical Mechanics* (American Mathematical Society, 1963).

[97] D. Redelmeier, Counting polyominoes: Yet another attack, Discrete Mathematics **36**, 191 (1981).